Palaeogeography, Palaeoclimatology, Palaeoecology 534 (2019) 109340

Contents lists available at ScienceDirect

Palaeogeography, Palaeoclimatology, Palaeoecology

journal homepage: www.elsevier.com/locate/palaeo

Dynamic surface-water alterations during sapropel S1 preserved in high-resolution shallow-water sediments of Taranto Gulf, central Mediterranean

Patrizia Maiorano[a,*], Maria Marino[a], Gert J. De Lange[b]

[a] Dipartimento di Scienze della Terra e Geoambientali, Università degli Studi di Bari Aldo Moro, Italy
[b] Department of Earth Sciences-Geochemistry, Faculty Geosciences, Utrecht University, the Netherlands

ARTICLE INFO

Keywords:
Core DP 30
Calcareous nannofossils
Primary productivity
Biogenic content preservation

ABSTRACT

The high sedimentation rate and shallow-water depositional depth of the sediments at site DP 30 in the Gulf of Taranto (central Mediterranean) provide unique biogenic signals that are usually not preserved in deeper records. This permits the reconstruction of long and short-term surface water modifications across the sapropel S1 period (10–6.5 ka), including calcareous nannofossil data at centennial-scale resolution.

The peculiar patterns of key taxa allowed the recognition of distinct long to short-term surface water changes that provide valuable evidence on climate conditions leading to sapropel deposition. As a long-term pattern, S1 is marked by a distinct increase of *Helicosphaera carteri*, thought to reflect increased detrital input/land-derived nutrients in the surface water, related to a higher influence of the Western Adriatic Current. A concomitant pattern of increased black organic particles in the sediments supports a connection between organic matter preservation at the seafloor and nutrient availability in the surface water. Decreased salinity in the surface water, testified by an increase of *Braurudosphaera bigelowii*, develops from 9.2 up to 6.5 ka.

At higher frequencies, additional changes occurred in surface-subsurface waters during the formation of S1 at shallow depths. Starting from 11 ka, the relative abundance pattern of *Florisphaera profunda* indicates a gradual nutrient enrichment in the subsurface waters and the development of a deep chlorophyll maximum (DCM), which becomes well established at the onset of sapropel S1, between 10 and 9 ka. A further change in the plankton ecosystem occurs between 9 and 8.2 ka, when reduced coccolithophore production is concomitant with diatom occurrence and enhanced Br/Ti level, implying a productivity increase. From 8 to 6.5 ka, coccolithophore productivity is re-established in relation to a reduction both in surface-water stratification and turbidity/nutrient availability, characterizing the final phase of sapropel formation. The turbidity in the surface waters was briefly reduced at 8.2 and 7.3 ka, when also oxygen conditions at the seafloor improved. A centennial variability in turbidity/low light conditions in surface waters is evident across S1 and is illustrated by the abundance patterns of *H. carteri* and *Gladiolithus flabellatus*. The occurrence of ascidian spicules also represents a distinct biotic signal across the S1 layer, indicating an increase of shallow-water biogenic carbonate or an aragonitic near-coastal source. Surface-water modifications at longer and shorter time scales, accompanying the deposition of sapropel S1 in the Gulf of Taranto, occurred nearly simultaneously and with a magnitude that is comparable to changes observed in S1 deposits in the central and eastern Mediterranean basin and slope settings.

1. Introduction

Sapropel S1 is the most recent among the organic-rich layers that periodically deposited in the eastern Mediterranean since the late Miocene (e.g. Olausson, 1961; Kidd et al., 1978; Emeis and Shipboard Scientific Party, 1996; Nijenhuis et al., 1996; Emeis et al., 1998). During the formation of S1, the eastern Mediterranean deep-sea basin has been predominantly oxygen free between 10.8 and 6.1 ka below 1.8 km (De Lange et al., 2008). This period is commonly associated with the Holocene African Humid Period (e.g. Rossignol-Strick, 1999; Gasse, 2002) and with lower salinity in the surface waters. The latter resulted from climate-related increased run-off including that from southern and northern borderlands of Mediterranean Sea. Increased southern borderlands' run-off during this period of enhanced monsoon regime in the equatorial African region was not only limited to enhanced Nile discharge but also the north-African river systems may have contributed (Rossignol-Strick et al., 1982; Rossignol-Strick, 1985; Howell and Thunell, 1992; Rohling et al., 2002, 2004; Wu et al., 2016, 2018).

* Corresponding author.
E-mail address: patrizia.maiorano@uniba.it (P. Maiorano).

https://doi.org/10.1016/j.palaeo.2019.109340
Received 20 February 2019; Received in revised form 29 July 2019; Accepted 17 August 2019
Available online 21 August 2019

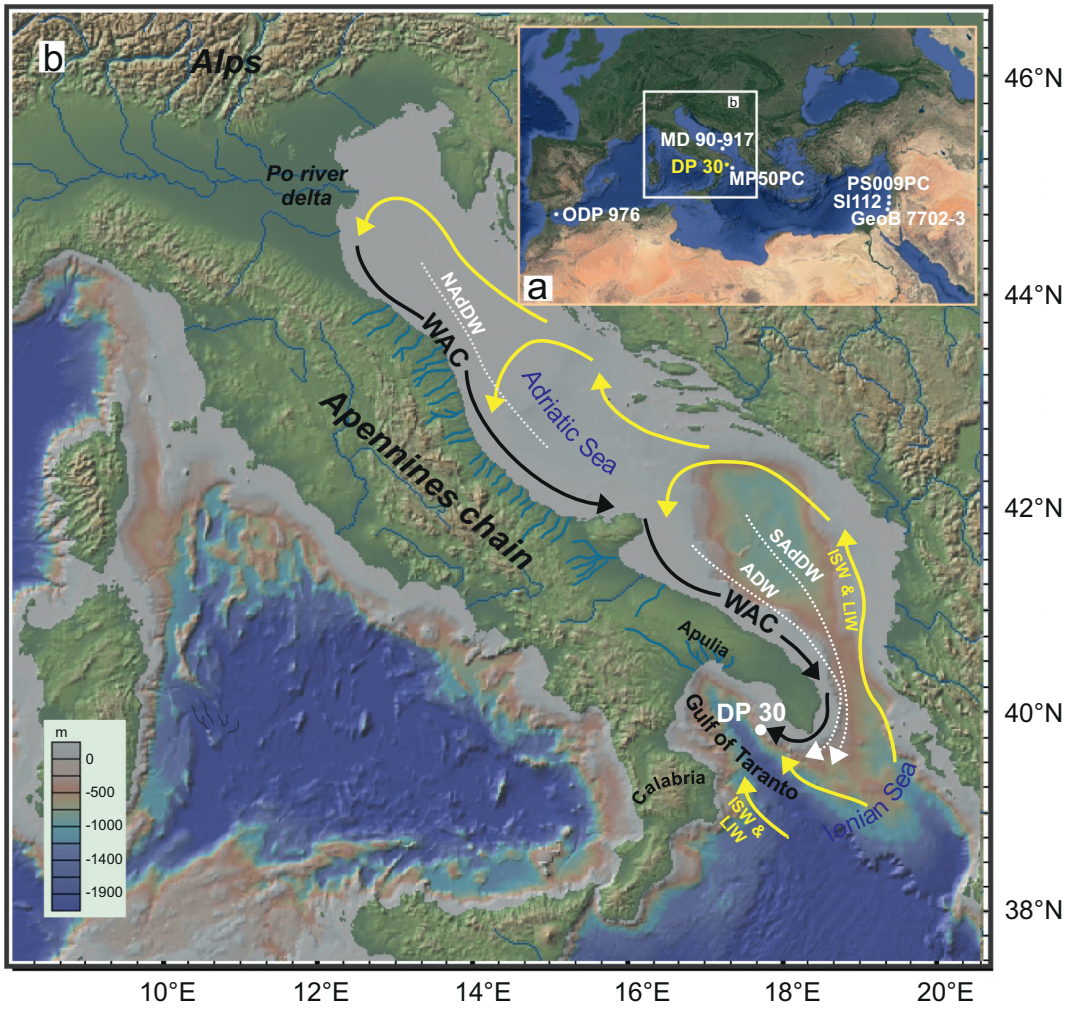

Fig. 1. a) Location map of core DP 30 and supplementary cores used for comparison and cited in the text. b) Adriatic and Gulf of Taranto general water masses circulation. WAC: Western Adriatic Current; ISW: Ionian Surface Water; LIW: Levantine Intermediate Water; ADW: Adriatic Deep Water; NAdDW: Northern Adriatic Dense Water; SAdDW: Southern Adriatic Dense Water.

Additional contributions came from the northern borderlands of the Mediterranean (Rossignol-Strick, 1987; Rohling and Hilgen, 1991; Rohling, 1994; Filippidi et al., 2016; Wu et al., 2016, 2018; Tesi et al., 2017; Filippidi and De Lange, 2019). Rainfall events over the northern Mediterranean borderland recorded during sapropel deposition have been correlated with the precession forcing acting on the north African monsoon activity (Toucanne et al., 2015), indicating a close coupling between low-and mid-latitude hydrological changes in the Mediterranean. The increased precipitation and the consequent reduced salinity in surface waters, caused low-density in the upper part of the water column, hampering eastern Mediterranean deep water formation and leading to the establishment of anoxic conditions at the seafloor (De Lange et al., 2008; Rohling et al., 2015). Increased river run-off also contributed to enhanced nutrients supply to the system, enhancing primary productivity (e.g. Rossignol-Strick, 1985; Kemp et al., 1999)- and shoaling of the nutricline with the establishment of deep chlorophyll maximum (DCM) (Castradori, 1993; Kemp et al., 1999; Rohling and Gieskes, 1989). Post-glacial freshening, driven by the inflow of less saline Atlantic waters via the Gibraltar strait, likely exerted an additional control on surface water stratification, vertical mixing and intermediate and deep-water formation, and on sapropel formation (Kotthoff et al., 2008; Spötl et al., 2010; Weldeab et al., 2014; Grimm et al., 2015; Toucanne et al., 2015; Grant et al., 2016). In areas other than the Levantine basin, such as the Adriatic Sea, the development of anoxic conditions seems lagged with respect to eastern Mediterranean records (Rohling et al., 1997, 2015). Recently, the oceanographic mechanism under which sapropels formed in this sector, which is close to the Gulf of Taranto, has been further investigated (Filippidi et al., 2016; Tesi et al., 2017; Filippidi and De Lange, 2019), focusing on high-resolution bottom-water proxies. The authors suggested that in the Adriatic Sea, anoxic conditions developed synchronously with the rest of the eastern Mediterranean. According to Tesi et al. (2017) the major eastern Mediterranean water-masses changes, due to enhanced monsoon precipitation, was a first-order driver on S1 deposition even on a larger-scale. Filippidi and De Lange (2019), analyzing southern Adriatic records retrieved at different water depth, provided direct proof for concomitant enhanced river run-off from northern and southern borderlands during deposition of S1. In the Gulf of Taranto, recent data from Di Donato et al. (2019) described the interval of S1 as extending between 10.2 ka and 7.8 ka and highlighted differences in the chronology of S1 interval between the Gulf of Taranto and the Ionian and Adriatic Sea. Despite the numerous studies, the exact mechanism for sapropel formation is still debated and high-resolution reconstructions of productivity variation and surface-water modifications outside the Levantine basin may improve the discussion on the basin- wide sapropel formation.

In this study we present a centennial-scale reconstruction of surface-water conditions accompanying the deposition of S1 as detected in the high sedimentation rate core DP30 in the Taranto Gulf, where no calcareous nannofossil data were available so far within S1. The core,

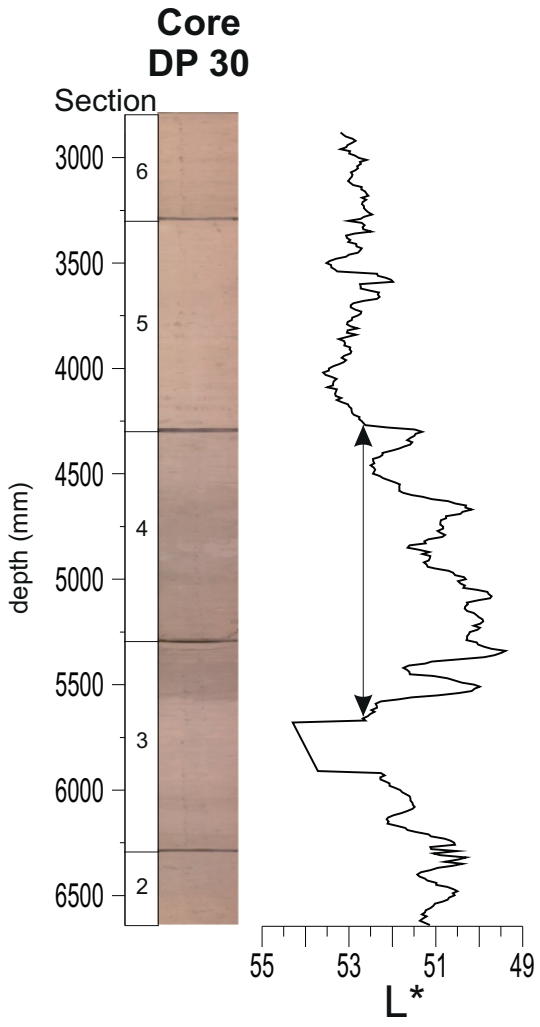

Fig. 2. DP 30 core photograph from the investigated interval and color lightness (L*) from Goudeau et al. (2014). Black arrow line indicates sapropel S1 according to Goudeau et al. (2014).

recovered at 270 m water depth, offers the opportunity to have insights on the environmental features occurring during deposition of S1 in a rather near-shore setting which, together with the high-quality recovery and high sedimentation rate is suitable in recording short-term modifications related to run-off, land-derived nutrients and variability of coastal currents. Our data set relies on new quantitative downcore coccolith variations and accompanying microfossil content (diatoms, siliceous sponges and ascidian spicules). All together these provide evidences on productivity, turbidity, and salinity variations in surface waters. Biotic proxies in core DP 30 are compared with geochemical data for the same core (Goudeau et al., 2014). Furthermore, we compare our surface water ecological variations data with the high-resolution patterns of organic and inorganic paleoenvironmental tracers across S1 observed elsewhere, in particular in the Levantine basin and central Mediterranean.

2. Oceanographic setting

The Gulf of Taranto is a deep semi-enclosed basin, surrounded by Calabria and Apulia and having lateral water exchange with the Ionian Sea (Fig. 1). In the area, the main drivers of surface circulation are the Western Adriatic Current (WAC) and the Ionian Surface Water (ISW). The WAC, is a less saline and nutrient-rich coastal current, flowing in a narrow band from the northern Adriatic Sea into the Gulf of Taranto (Poulain, 2001; Bignami et al., 2007; Turchetto et al., 2007). Its primary fluvial contribution is the Po River in the north, while additional minor contributions come from many smaller Alpine and Apennines rivers flowing into the northern Adriatic Sea (Turchetto et al., 2007). The WAC has a significant interannual variability and its influence along the southern Italian coast and the Gulf of Taranto is higher during winter and spring (Poulain, 2001; Milligan and Cattaneo, 2007), while it is weaker during summer due to the reduced river discharge. The WAC is responsible for sediment supply coming from the Po River (the Adriatic mud belt) as far south as the eastern Gulf of Taranto (Goudeau et al., 2013). Detailed geochemical studies in the Gulf of Taranto, dealing with the Late Holocene portion of core DP 30 (Goudeau et al., 2014, 2015) as well as of other cores from the same location (Grauel et al., 2013a, 2013b), revealed how the area records high frequency variations in the strength of the WAC and of ISW in response to climate variability. Specifically, on decadal to multicentennial temporal scale, warm and wetter conditions in the Gulf of Taranto promoted increased dominance of the WAC, throughout increased precipitation and enhanced outflow of the Po River and Apennines rivers (Fig. 1); while increased influence of the more saline water from ISW occurred during cold-dry conditions (Grauel et al., 2013b).

At present, the fluvial input plays a crucial role in nutrient supply and drives the primary productivity of the Adriatic Sea (e.g. Boldrin et al., 2005). In the Gulf of Taranto, the WAC mixes with the warmer and more saline ISW, which enters the Gulf of Taranto from the south (Fig. 1). At mid water depth, between 200 and 600 m, the Levantine Intermediate Water (LIW) flows from the central Ionian Sea into the Gulf of Taranto (Malanotte-Rizzoli et al., 1997; Sellschopp and Álvarez, 2003). The bottom waters are characterized by the Adriatic Deep Water (ADW), a dense water mass formed by the Northern Adriatic Dense Water (NAdDW) and Southern Adriatic Dense Water (SAdDW). The NAdDW results from sustained NE Bora wind events during winter in the northern Adriatic Sea (Turchetto et al., 2007). It flows southward and can be observed in the southern Adriatic Sea during spring (Grbec et al., 2007; Turchetto et al., 2007). The SAdDW derives from deep convection during late winter/early spring in the southern Adriatic Sea (Artegiani et al., 1997; Vilibić and Orlić, 2002).

3. Material and methods

3.1. Core material and chronology

The piston core DP 30 (39°83 N, 17°80 E, 270 m water depth) was retrieved during RV *Pelagia* cruise 'DOPPIO' in 2008 from the Apulian Margin, a wide continental shelf having a slight depth gradient towards the deep Taranto Valley (Rossi et al., 1983). Grain size and geochemical features are discussed in detail in Goudeau et al. (2013, 2014) to which we refer. Total core length is 8.28 m and the interval investigated in this study extends from about 6.5 to 3 m (Fig. 2). Sediments are rather homogeneous and predominantly consist of light gray–brown silty-clays. The sediments also include an interval of ~1.4 m thick, that is characterized by an increase in black particles corresponding to sapropel S1 as indicated in Goudeau et al. (2014). Changes in sediment color have been measured by means of Spectrophotometer core scanner (Goudeau et al., 2014) as shown in Fig. 2 and are here used to trace the S1 layer. For the studied interval we follow the age model by Goudeau et al. (2014) based on ^{14}C calibration from 7 evenly spaced data points between 3.63 and 15.65 cal ka.

3.2. Calcareous nannofossil and auxiliary microfossil analyses

From core section 2 to 6, corresponding to the 664 to 287 cm core depth interval, 96 samples were analyzed at 4 cm spacing, providing a temporal resolution of 80–90 years. Slides for calcareous nannofossil analysis were prepared according to the method of Flores and Sierro (1997) to estimate absolute coccolith abundances. Quantitative

analyses were performed using a polarized light microscope at 1000× magnification. Abundances of all the taxa were firstly determined by counting at least 300 coccoliths of all sizes in a variable number of fields of view, ranging between about 15 and 50. Reworked calcareous nannofossils were counted separately in the investigated fields of view and their relative % abundances were determined against the 300 non-reworked coccoliths. A supplementary counting was then performed to estimate abundance of uncommon taxa (having abundances < 5%) relative to about 1000 coccoliths, in order to reduce the standard error associated to the counting. Variations in the assemblage are estimated using relative abundances, while absolute coccolith abundances are expressed as total number of coccoliths/g of sediment. Quantitative data were collected on about 20 taxonomic units and species identification follows Young et al. (2003) and Jordan et al. (2004). Only selected taxa, showing relevant variations are plotted for paleoenvironmental interpretation.

Abundances of diatoms, siliceous sponge and ascidian spicules have been estimated using plane polarized light. No taxonomic identification has been performed within these groups, however their abundances have been estimated in 150 fields of view and plotted as number of specimens/g of sediment.

3.3. Key taxa for paleoenvironmental reconstruction

The cumulative percentages of calcareous nannofossils *Syracosphaera pulchra*, *Umbellosphaera* spp., *Discosphaera tubifera*, *Rhabdosphaera clavigera*, *Umbilicosphaera* spp., *Oolithotus fragilis*, are considered as warm-water proxy and labeled as Warm water taxa (Wwt) according to their ecological preferences for tropical-subtropical surface waters (Winter et al., 1994; Baumann et al., 2004; Boeckel and Baumann, 2004).

The taxon *Helicosphaera carteri* has been associated to turbid uppermost waters (Colmenero-Hidalgo et al., 2004; Grelaud et al., 2012) and high nutrient content in waters between 40 and 70 m (Cros et al., 2000). Accordingly, we consider the abundance of this taxon as a proxy for detrital input/turbidity in surface water and moderately elevated nutrient content. Although with different temporal resolution and variable interpretation, the proliferation of the taxon has been previously recorded during sapropel deposition, in the Adriatic (Narciso et al., 2010, 2013), Ionian (Negri et al., 1999; Negri and Giunta, 2001) and Levantine basins (Corselli et al., 2002; Principato et al., 2006; Grelaud et al., 2012).

The deep dwelling species *Florisphaera profunda* is used as a proxy for identification of Deep Chlorophyll Maximum (DCM) (Castradori, 1993). The latter is a highly productive layer in the lower part of the photic zone, related to density stratification and shoaling of intermediate waters and of the pycnocline to 50 to 120 m during sapropel events (Rohling and Gieskes, 1989; Myers et al., 1998). The establishment of a DCM is a known feature during deposition of sapropel layers (e.g. Castradori, 1992, 1993; Negri et al., 1999; Negri and Giunta, 2001; Corselli et al., 2002; Principato et al., 2003; Thomson et al., 2004; Triantaphyllou et al., 2010; Incarbona et al., 2011; Grelaud et al., 2012). *Brarudosphaera bigelowii* is used as a proxy for lower salinity in surface water (Gran and Braarud, 1935; Bukry, 1974; Negri and Giunta, 2001; Hagino et al., 2005; Giunta et al., 2007). Maximum abundance of *G. flabellatus* is usually recorded at a depth well below that of the deep-dweller *F. profunda* and cell numbers reach a maximum at low solar irradiance level (Poulton et al., 2017). The ecology of *G. flabellatus* is poorly known and its abundance pattern is rarely documented during sapropel times. This is due to its reduced abundance related to its generally high potential for dissolution (Giunta et al., 2006; Principato et al., 2006).

3.4. Paleoclimate proxy records used for comparison

The high resolution alkenone based SST from the ODP Site 976 in the Alboran Sea (Martrat et al., 2014), TEX_{86}SST from GeoB 7702-3 (Castañeda et al., 2010), together with $\delta^{18}O_{G.\ ruber}$ at core PS009PC (Hennekam et al., 2014) in the Levantine Basin are plotted with selected biotic proxies obtained at Core DP 30 to compare the main regional climate evolution occurring in the studied interval. Moreover, in order to test to what extent the shallow-water S1 in the Taranto Gulf correlates to the basin-wide deposition of S1, we compared the acquired dataset with few high-resolution geochemical proxies. The latter have been chosen in order to provide a comparison with different Mediterranean records under the influence of freshwater supply from southern and northern Mediterranean borderlands. Specifically, we referred to the $Ba/Ca_{G.\ ruber}$ ratio from the Levantine Basin Core SL112 (Weldeab et al., 2014), a surface water proxy which primarily reflects the degree of Nile-water related freshening of the Levantine surface waters in response to the east African monsoon. In addition, total organic carbon (TOC) and V/Al bulk ratio from core PS009PC (Hennekam et al., 2014) are also considered as indicative of bottom water redox conditions and as being valuable records for multicentennial modification within S1 in the Levantine basin. TOC content from the southern Adriatic Sea core MP50PC (Filippidi et al., 2016) is also considered as well as the $\delta^{18}O_w$ from the Adriatic Sea core MD 90-917 (Siani et al., 2013) since these core locations are under the influence of fresh water discharge from a northern borderland source.

4. Results

At core DP 30, the calcareous nannofossil assemblages are mainly composed of *E. huxleyi*, representing 70–80%, but not showing any important abundance variation (Fig. 3a). Subordinate taxa, showing distinct patterns throughout the core and specifically during S1 are Wwt (Fig. 3b), *H. carteri*, *G. flabellatus*, *B. bigelowii*, (Fig. 4b–d), and *F. profunda* (Fig. 5c). On the other hand, *Coccolithus pelagicus* s.l., *Calcidiscus leptoporus* s.l., *Gephyrocapsa* spp., *Coronosphaera* spp. (not shown) are extremely rare or do not display significant variations. The oldest part of the investigated record, between 12.5 and 11.8 ka, is marked by very low relative abundances of Wwt (Fig. 3b) and enhanced reworked coccoliths, the latter reaching relative abundances of 20% (Fig. 3c). Gradual increase of Wwt, from relative abundance of 1% to 3% occurs between 11.8 and 10 ka (Fig. 3b), up to 6–8% upwards. Between 10 and 6.5 ka, which is the interval of S1 deposition, the biotic proxies record abundance variations at centennial to millennial scale and are summarized in Figs. 4-5. Relative abundance of *Helicosphaera carteri* increases to values > 1% between 12.5 and 11.8 ka and across S1, between 10 and 6.5 ka. In more detail, a prominent increase of the taxon, with relative abundance exceeding values of 2%, coincides with the earlier portion of S1, between 9.5 and 8.4 ka. From 6.5 ka upwards, the relative abundance of *H. carteri* decreases to values lower than 1%. Across the whole S1, *G. flabellatus* (Fig. 4c) has long-term pattern comparable to that of *H. carteri* (Fig. 4b) and both the taxa also display similar multicentennial variations. *Florisphaera profunda* gradually increases to values > 8%, starting from about 11 ka and following the deglaciation; maximum relative abundances of the taxon characterize the lowermost part of S1 (Fig. 5c), specifically between 10 and 9.1 ka. Within the remaining part of S1, *F. profunda* decreases, showing relative abundances often < 8%, with the exclusion of few abundance peaks. *B. bigelowii*, although always rare in the assemblage, increases from 9.2 ka up to 6.4 ka. Total coccolith abundance pattern shows a long-term increasing trend from the oldest part of the record upwards, although a marked decreasing interval is observed between 9.3 ka and 8.1 ka (Fig. 5b). Diatoms are absent along most of the record (Fig. 5e); however their occurrence, although characterized by low abundances, is clearly concomitant with the decrease of the total coccolith abundance. Increase in abundance of siliceous sponges and ascidian spicules characterizes all S1 interval (Fig. 5f–g).

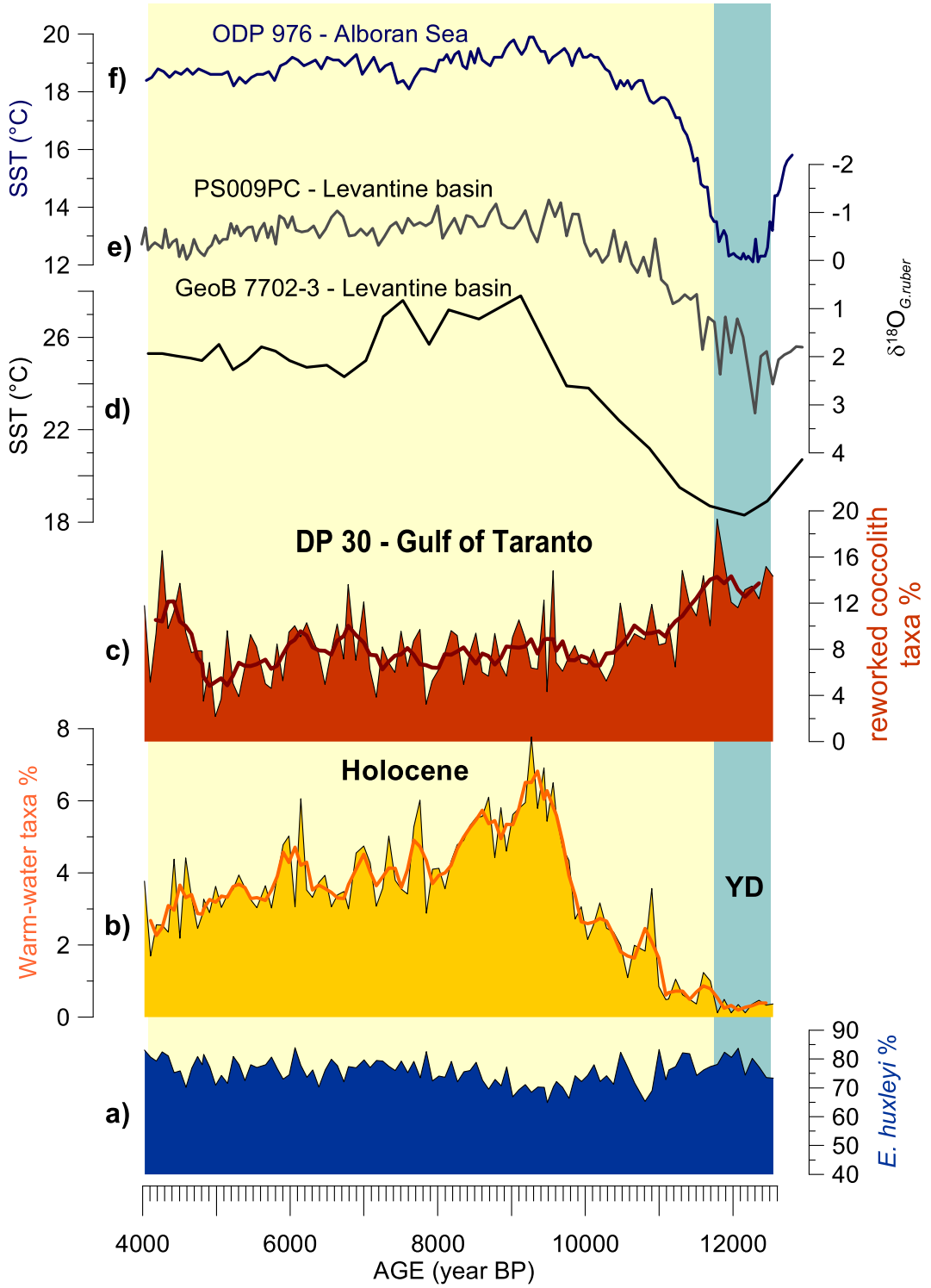

Fig. 3. Dominant (a), climate sensitive (b) and reworked (c) coccolith taxa at core DP30. Warm water and reworked taxa are plotted as three-point moving averages. SST from core GeoB 7702-3 (d) (Castañeda et al., 2010) and ODP Site 976 (f) (Martrat et al., 2014), and $\delta^{18}O$ (e) from core PS009PC (Hennekam et al., 2014) are also shown for comparison. YD: Younger Dryas.

5. Discussion

The oldest portion of the investigated interval (12.5–11.8 ka) is marked by very low relative abundances of Wwt (Fig. 3b), tracing cold surface water conditions characterizing the Younger Dryas Stadial (YD). Reworked coccoliths (Fig. 3c), which provide information on erosion-transport processes deriving from areas surrounding the sedimentary basin (Flores et al., 1997; Ferreira et al., 2008; Bonomo et al., 2014), also increase in the same interval. This evidence suggests increased erosion on land and enhanced terrigenous input into the basin, likely induced by drier conditions on land during the deglaciation in central Mediterranean (Desprat et al., 2013). The correlation with SST Mediterranean records from both the eastern Levantine basin (Fig. 3d) and the western Alboran Sea (Fig. 3f) sustains, in this portion of the core,

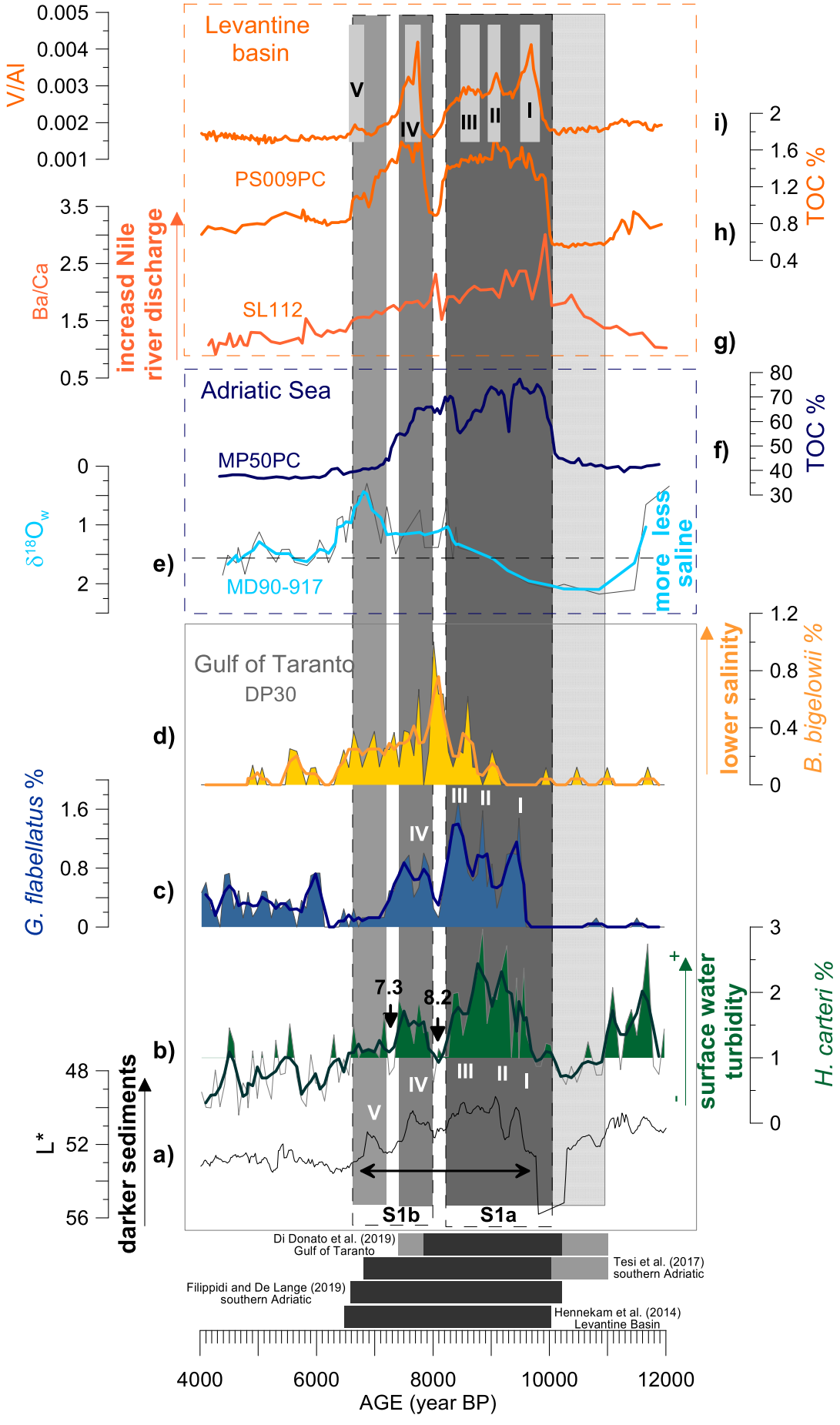

(caption on next page)

Fig. 4. Color lightness (L*) (a) and biotic proxies (b-d) at core DP 30 plotted as all data and three-point moving averages, compared with surface and bottom water signals from central and easternmost Mediterranean basin (e-i) and Adriatic surface salinity proxy: $\delta^{18}O_w$ (e) (Siani et al., 2013) dashed line corresponds to modern $\delta^{18}O_w$ values in the South Adriatic after Pierre (1999); Adriatic bottom water proxy: TOC (f) (Filippidi and De Lange, 2019); Nile run-off proxy: Ba/Ca of *G. ruber* (g) (Weldeab et al., 2014); bottom water redox condition tracers: TOC and V/Al (h, i) (Hennekam et al., 2014). Black arrow line on Color lightness (L*) indicates sapropel S1 according to Goudeau et al. (2014). Grey bands highlight main changes in surface waters across S1. Vertical dotted rectangle traces the phase of pre-sapropel deposition as marked by the increase of *F. profunda* as shown in Fig. 5c. Multicentennial variations in surface and bottom water proxies are marked as I–V following Hennekam et al. (2014). Horizontal dark grey bars indicate duration of Sapropel 1 (S1) as recorded by several studies in the easternmost and central Mediterranean Sea, while horizontal light grey bars indicate transitional/pre-sapropel phases. Green area for the % of *H. carteri* indicates relative abundances > 1% which characterize sapropel S1. Slight difference in the chronology of mid-S1 interruption between cores DP 30 and MP50PC is within uncertainties of comparing independent ages and samplings. (For interpretation of the references to color in this figure legend, the reader is referred to the web version of this article.)

the identification of the Younger Dryas, ending at ~11.8 ka. On the other hand, the gradual increase of Wwt between 11.8 and 10 ka (Fig. 3b) marks the transition into the early Holocene. The main variations in the abundance of biotic proxies and in surface-water conditions are recorded between 9.8 and 6.5 ka (Figs. 4–5). This interval is nearly coincident with the identification of S1 proposed in Goudeau et al. (2014) at the same core recorded between 9.8 and 6.8 ka. However, the first subtle increase of *H. carteri*, observed at 10 ka, indicates that surface water perturbations, accompanying S1 deposition, slightly predated the enhanced organic matter flux/preservation at the sea floor of about 200 years. Interval of modification in surface water is practically synchronous with deposition of S1 in Adriatic (Tesi et al., 2017; Filippidi and De Lange, 2019), with slight offset in timing likely within uncertainties of comparing independent ages and samplings (Fig. 4) and also with eastern Mediterranean records (De Lange et al., 2008; Hennekam et al., 2014) (Fig. 4h–i). In this interval, which is the main focus of this study, the dominant taxon *E. huxleyi* does not show any relevant variation as throughout the record and therefore is not helpful for paleoenvironmental reconstruction. On the other hand, few taxa (Figs. 4–5), although representing minor components of the assemblage, display distinct fluctuations and appear to be diagnostic for identification of environmental changes that have occurred in surface water immediately before, during, and after sapropel S1 deposition as discussed below. Some of these taxa are documented in the literature as being very prone to dissolution, thus often are barely present -if at all- in deeper seated S1 sediments. This is the case for example of *G. flabellatus* (Giunta et al., 2006; Principato et al., 2006) and of the diatom content into the sediments (e.g. Malinverno et al., 2014). Consequently, DP30 core site not only provides sediments with high-accumulation rates but also with excellent preservation.

5.1. Turbidity, freshwater flooding and preservation of organic fluxes

Among calcareous nannofossil surface water proxies, the increase in the relative abundance of *H. carteri* (Fig. 4b) is one of the most distinct signals across S1 in core DP 30. The quantitative distribution of the taxon is very similar to the L* pattern (Fig. 4a), even at short-term scale, and suggests a strong coupling between surface water conditions and organic matter flux/preservation at the seafloor. These features support identification of multiple phases within S1, S1a and S1b (sensu Rohling et al., 1997), spanning 10–8.2 ka and 8–6.5 ka intervals, respectively and not previously identified at core DP 30. The latter interval is characterized by a twofold subdivision (Figs. 4–5). We consider the behavior of *H. carteri* as the response to enhanced detrital input/land derived nutrients imported in surface water, during a phase of enhanced run-off accompanying deposition of S1 (Rossignol-Strick et al., 1982; Rossignol-Strick, 1987; Rohling, 1994; Rohling and Hilgen, 1991; Rohling et al., 2002; Marino et al., 2009; Weldeab et al., 2014; Hennekam et al., 2014). Specifically, higher influence of the nutrient-rich WAC and of the Adriatic mud belt can be inferred at the core location during this phase. The concomitant highest values in black organic particles (Fig. 4a), relates to enhanced nutrients and organic matter input during higher run-off.

The long-term trend of *H. carteri*, across the whole S1 is rather well comparable to the pattern of the Ba/Ca ratio measured on *Globigerinoides ruber* (Fig. 4g) in the eastern Mediterranean (Weldeab et al., 2014), a measure of changes in in monsoon freshwater discharge via Nile River (Weldeab et al., 2014). These results, therefore, suggest a common climate-related response between monsoon-derived precipitation/run-off in the eastern Mediterranean region and that in the Taranto Gulf, the latter having a northern Mediterranean borderland source. This evidence is in favor of the hypothesis of the relationship between the increased storm track precipitation affecting the northern Mediterranean borderlands with that of the north African summer monsoon during sapropel deposition (Toucanne et al., 2015). A simultaneous occurrence between increased northern and southern borderlands run-off has been also recently reported in the south Adriatic Sea (Filippidi and De Lange, 2019) during sapropel S1, while not yet documented so far in the Gulf of Taranto.

Looking in more detail, the increase of *H. carteri* starts at 9.8 ka and reaches maximum values not before than 9.2 ka. From that time onward, the distribution of *B. bigelowii* (Fig. 4d) indicates decreased salinity levels up to 6.4 ka. This episode appears a feature of the central Mediterranean during deposition of S1, as indicated by the similar pattern between *B. bigelowii* at the studied site and the $\delta^{18}O_w$ from the Adriatic Sea (Siani et al., 2013) (Fig. 4e). Considering the core location, it suggests enhanced influx of fresh water from the northern borderlands which is also consistent with enhanced regional rainfall starting from ca. 8.9 ka (Zanchetta et al., 2007).

The distinct reduction in surface-water turbidity/high nutrients indicated by the relative abundance drop of *H. carteri* at 8.2 ka is consistent with the mid-S1 interruption (Rohling et al., 1997; De Rijk et al., 1999; Mercone et al., 2000; Casford et al., 2003; De Lange et al., 2008; Almogi-Labin et al., 2009; Hennekam et al., 2014; Rohling et al., 2015; Filippidi et al., 2016; Tesi et al., 2017; Filippidi and De Lange, 2019), related to a brief cooling event in the Northern Hemisphere (Rohling and Pälike, 2005). The latter resulted in surface waters cooling in the northern part of the eastern Mediterranean and subsequent temporary reactivation of bottom water formation and cessation of sapropel formation (e.g. Rohling et al., 1997, 2015; Mercone et al., 2001; Casford et al., 2003). This is documented by several geochemical eastern Mediterranean bottom-water ventilation proxies partly shown in Fig. 4f, h–i. While the temporary re-ventilation interrupting S1 deposition is particularly evident over basin and slope sediments in eastern and central Mediterranean, it seems not well-recorded by bottom-water proxies at shallower depths in the mid-Adriatic depression at 260 m depth (Tesi et al., 2017). On the other hand, it appears well-recorded at our studied site, by surface water proxies and specifically by temporary reduction in relative abundance of *H. carteri*. The latter is also concurrent with a decreased flux/preservation of organic matter during a drier climate phase, as suggested by the color lightening (Fig. 4a), thus indicating that this northern borderland 'cold event', affected both the surface and bottom environment at shallow water depth. This may be related to the fact that core DP 30, located in a rather nearshore setting in the Taranto Gulf, is well suited to record variation of the intensity of the WAC and of the Adriatic mud belt. The sapropel interruption did not affect the distribution of *B. bigelowii* as also observed in the Adriatic Sea records (Giunta et al., 2003; Narciso et al., 2013). This suggests that no major salinity variation co-occurred, which is consistent with the $\delta^{18}O_w$ profile from the Adriatic Sea (Siani

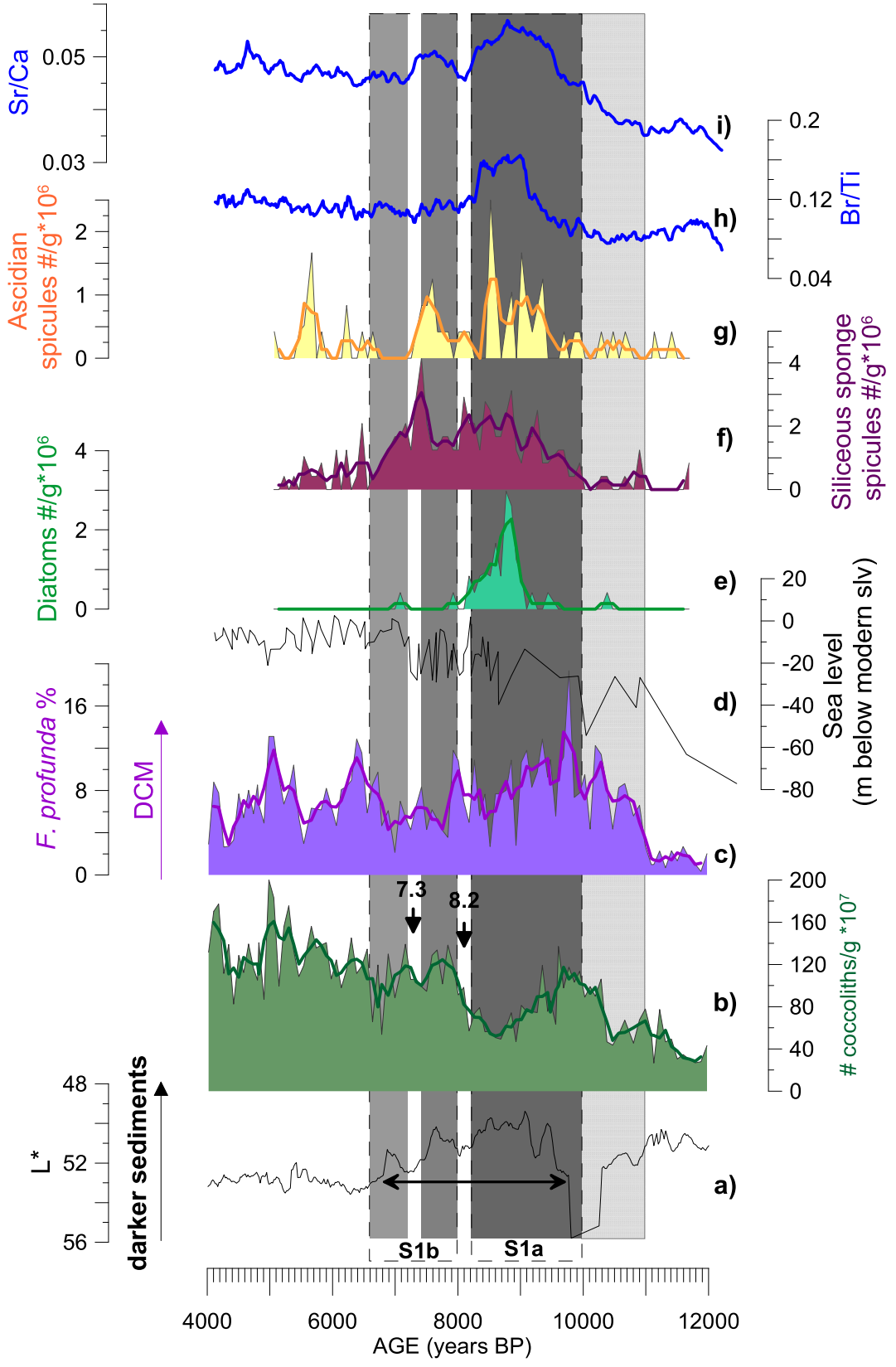

Fig. 5. Sediment color variations, microfossils absolute and relative abundances (all data and three-point moving average), and geochemical ratios for sediments in core DP30. (a) Color lightness (L*); (b) total coccolith abundance (# of coccoliths/g of sediment); (c) relative abundance of *F. profunda*; (d) pattern of sea level variability (Grant et al., 2012); (e) diatoms (# of specimens/g of sediment); (f) siliceous sponges (# of specimens/g of sediment); (g) ascidian spicules (# of specimens/g of sediment); (h) Sr/Ca and (i) Br/Ti (both plotted as ratio of counts from Goudeau et al., 2014). Black arrow line on Color lightness (L*) indicates sapropel S1 according to Goudeau et al. (2014). Grey bands highlight main changes in surface waters across S1. Vertical dotted rectangle traces the phase of pre-sapropel deposition as marked by the increase of *F. profunda*.

et al., 2013) (Fig. 4e).

After sapropel interruption, relative abundance of *H. carteri* increased again up to ca. 6.5 ka, although values were lower than in S1a, impling a reduction in turbidity/flooding with respect to S1a which is also concomitant to a decline in the amount of black particles (Fig. 4a). This pattern characterizes S1b and parallels the progressive weakening of east African monsoon precipitation and associated runoff (Fig. 4g), and of decreasing organic matter preservation in the southern Adriatic (Fig. 4f; Filippidi et al., 2016; Filippidi and De Lange, 2019). In addition, the slight and brief reduction of *H. carteri* at ca. 7.3 ka, and of the L* pattern (Fig. 4a), could be a signal of a supplementary short-lived reduction of river run-off, which correlates well with a second cooling and arid spell and rapid improvement of deep-water oxygen conditions recorded in the southern Adriatic (Filippidi et al., 2016; Tesi et al., 2017). The event is largely recorded in several continental and marine records (e.g. Bar-Matthews et al., 2000; Gasse, 2000; Frisia et al., 2006; Constantin et al., 2007; Kuhnt et al., 2007; Magny et al., 2011; Triantaphyllou, 2014; Triantaphyllou et al., 2016) and, similarly to the 8.2 ka interruption event, is associated with the northern borderland climate system and a weakening in North Hemisphere summer insolation (Bond et al., 2001). Lower relative abundances of *H. carteri* between 7.3 and 6.5 ka mark the last subtle turbidity/run-off signature in surface water, coeval with the decline of the L* pattern (Fig. 4a) and accompanying the final phase of S1b. A concomitant recovery of seafloor ventilation in the Taranto Gulf is accordingly documented by benthic foraminifera assemblages, starting from 7.3 ka (Di Donato et al., 2019) and therefore of the restoration of ADW in the area. This phase is simultaneous to the changes leading to termination of S1 deposition both in the eastern and central Mediterranean (Hennekam et al., 2014; Filippidi et al., 2016; Filippidi and De Lange, 2019), as marked by diminished organic matter content (Fig. 4f, h) and by lower concentrations of redox-sensitive elements (Fig. 4i), thus indicating a remarkable similarity in timing and magnitude of the end of S1 in such different environmental settings.

5.2. Multicentennial variability in sea surface and bottom environments

Four multicentennial phases (phases I-IV) showing distinct increases of *H. carteri* (Fig. 4b) as well as five increases in L* (Fig. 4a) are observed across S1, suggesting a high-frequency correlation between increased surface water turbidity/river input and enhanced export productivity/preservation of organic matter at the seafloor. The pattern of *G. flabellatus* closely resembles the *H. carteri* abundance fluctuations and this is thought to reflect a common preference of both taxa for a turbid upper water layer. This is in agreement with maximum abundance of *G. flabellatus* at low solar irradiance level and with its possible alternative nutritional strategies than autotrophy (i.e., mixotrophy or phagotrophy) (Poulton et al., 2017). We assume that at site DP30, increased turbidity in surface waters, as well as organic matter deriving from land during enhanced run-off, would have provided suitable turbid/nutrient-rich surface water conditions for *H. carteri* and, at the same time, favorable low-light conditions and/or alternative food resources promoting proliferation of *G. flabellatus* during phases I-III in S1a and phase IV in the lower part of S1b (Fig. 4c).

The multicentennial changes recorded by *G. flabellatus*, *H. carteri* and L* recall those observed in the eastern Mediterranean by means of recurrent increases in V/Al ratio (phases I-V in Fig. 4i). These are thought to be a response to solar-driven variability in Nile discharge during sapropel deposition (Hennekam et al., 2014). Variability in solar irradiance has also been reported as the driving force for the redox-sensitive elements variability/ventilation in the Ionian Sea during S1 (Jilbert et al., 2010). For core DP 30, the younger of the multicentennial fluctuations ("V" in Hennekam et al., 2014; Fig. 4i) is recorded between 7.2 and 6.5 ka and highlighted by the last and less intense peak in L* pattern and a last step in the occurrence of *H. carteri* (Fig. 4b), although with lower relative abundance values with respect to previous phases. This pattern suggests a further reduction in turbidity/nutrient content in surface water, which likely resulted in reduced organic carbon flux at the sea floor. Phase V is less intense in Hennekam's geochemical records as well (Fig. 4h–i) and is also concomitant with the gradual decreasing pattern of TOC content in the southern Adriatic record of Filippidi and De Lange (2019) (Fig. 4g) for the intermediate water 775-m site, supporting a gradual shift to sapropel termination and return to background conditions. The overall calcareous nannofossil data in core DP 30 support a multicentennial variability across S1 is surface water proxies as well, and allow extending Hennekam's hypothesis to a larger Mediterranean scale. In the latter hypothesis, the higher-amplitude variability of solar activity on Indian Ocean-derived precipitation, affected the Nile discharge variability during S1 deposition. This feature modulated nutrient inputs and intermediate water ventilation in the eastern Mediterranean, thus affecting productivity and redox conditions on multicentennial time scales during S1 deposition. Considering that, at the core location, run-off/freshwater supply has essentially a northern source, it is noteworthy the relationship highlighted by previous studies between Alpine flood variability/precipitation and solar irradiance during the Holocene (Wirth et al., 2013). The latter link appears well supported by the DP30 dataset during S1 formation.

5.3. Short-term productivity changes: calcareous versus siliceous fluxes

The pattern of *F. profunda* at site DP30 indicates the establishment of deep nutricline in the lower photic zone and the development of a DCM (for reference refer to Section 3.3). The latter actually occurs as a gradual phenomenon as indicated by a continuing increase of the taxon starting at about 11 ka (Fig. 5c) and culminating between 10 and 9.1 ka. This pattern appears in relation with climate amelioration and sea level rise occurring at the deglaciation phase (Fig. 5c,d), leading to water-column stratification, supporting the hypothesis that sea level rise, together with fresh water discharge, contributed to surface-water buoyancy changes and to S1 deposition (Grimm et al., 2015; Grant et al., 2016). A gradual onset of a DCM has been documented in the eastern Mediterranean during S1 (Principato et al., 2003; Triantaphyllou et al., 2009; Incarbona and Di Stefano, 2019) as well as during S5 (Corselli et al., 2002). Other studies indicate the abrupt occurrence of deep nutricline concomitant with the sapropel base (Castradori, 1993; Negri et al., 1999; Incarbona et al., 2011). The gradual increase of *F. profunda* at core DP 30 appears concurrent with the transitional/pre-sapropel deterioration of bottom oxygen levels recorded in deeper settings between about 11 and 10 ka in the southern Adriatic (Tesi et al., 2017) and Gulf of Taranto (Di Donato et al., 2019) (Fig. 4). The increase of *F. profunda* is not persistent for the whole duration of S1, likely to be related to short-term productivity modifications in the photic layer discussed below and to variation in surface water stratification. In fact, in the second half of S1a, between 9.1 and 8.3 ka, the sharp decrease in *F. profunda* and in the total coccolithophore concentration coincides with the occurrence of diatoms (Figs. 5e; 6_{1-2}). This evidence provides a documentation for the reversal abundances between coccolithophores and diatoms during sapropel deposition, which represents an interesting topic, not well documented in the vast sapropel literature. In fact, a coccolithophore productivity decrease during sapropel, in favor of the more competitive diatoms, has been suggested in previous studies mainly relying on the low coccolith concentrations (van Os et al., 1994; Negri et al., 1999; Negri and Giunta, 2001; Principato et al., 2006; Grelaud et al., 2012). An observed shift between diatoms/coccoliths occurrence has been documented only for S5 (Corselli et al., 2002; Giunta et al., 2006). This is due to the low preservation of the opaline skeleton and to the rarity of the siliceous plankton preservation in highly silica-undersaturated Mediterranean waters (Krom et al., 1991; Cramp and O'Sullivan, 1999) or to the scarcity of silica and phosphorus, the main nutrients for diatom growth (Ludwig and Volcani, 1986). Data from the present-day export production in the Ionian Sea (Malinverno et al., 2014) indicate that diatom fluxes are rather low if compared with

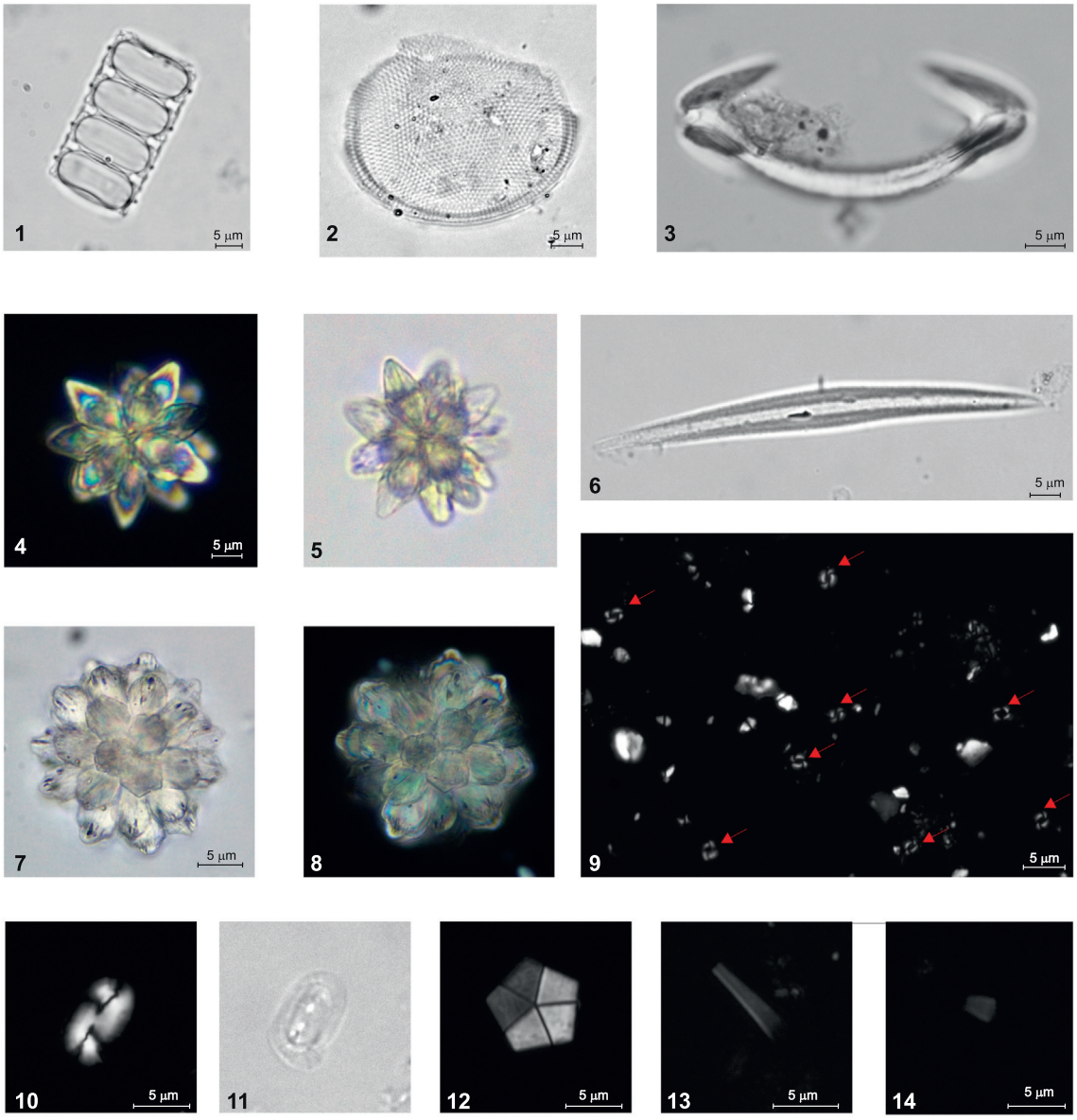

Fig. 6. Polarized light images of selected biogenic content occurring during S1 at core DP 30.
XP: crossed polarized light; PL: plane polarized light. 1-2: Diatoms, PL. 3, 6: sponge spicules, PL. 4-5, 7-8: ascidians, 4,8 XP; 5,7 PL 9: red arrows indicate specimens of the dominant taxon *Emiliania huxleyi* (Lohmann), XP. 10-11: *Helicosphaera carteri* (Wallich), 10 XP, 11 PL. 12: *Braarudosphaera bigelowii* (Gran and Braarud), XP. *Gladiolithus flabellatus* (Halldal and Markali), XP. *Florisphaera profunda* (Okada and Honjo), XP. (For interpretation of the references to color in this figure legend, the reader is referred to the web version of this article.)

more eutrophic pelagic settings of the world oceans, with dissolution occurring within the bottom sediments, where diatoms are not preserved. At site DP 30, siliceous skeletons are preserved all through the S1 and mainly consist of sponge spicules (Figs. 5g, $6_{3,6}$) and partially of diatoms (Figs. 5e, 6). The occurrence of other siliceous microfossils, during the full S1 (Fig. 5), suggests that selective diatom/opaline preservation did not play a dominant role at the core location, thus, the diatom signature reflects a primary signal. The siliceous content is likely to be related to enhanced continental input and nutrient content in surface water, fresh water discharge and surface water stratification (Sancetta, 1994; Kemp et al., 1999; Corselli et al., 2002), and to the high sedimentation rate, which together provide favorable conditions for the preservation of siliceous microfossils. The more opportunistic diatoms were responsible for the highest productivity phase between 9 and 8.2 ka, and for the reduced coccolithophore production, including that for the deep-dweller taxon *F. profunda*. The highest productivity, in the second half of S1a, is also marked by the coeval drastic increase of the Br/Ti ratio in these sediments (Fig. 5h), the Br being a geochemical proxy for marine organic matter (Ziegler et al., 2008; Goudeau et al., 2014). Increase in the Br/Ti ratio also coincides with enhanced turbidity and the onset of reduced salinity as indicated by highest abundances of *H. carteri* and *B. bigelowii* respectively (Fig. 4b, d).

The 8.2 event marks the cessation of diatom occurrence, likely due to interruption of the stratification and reduced nutrient supply at the site location. Subsequently, during S1b, the distinct increase of total coccoliths (Fig. 5b) indicates a re-establishment of coccolithophore productivity in surface water to be expected in relation with the reduced fresh water discharge and nutrient availability characterizing S1b, thus restoration of more favorable surface water condition for the whole coccolithophore assemblage. The low abundance of *F. profunda* during this phase (Fig. 5c) indicates a reduction in surface water stratification.

Modification in the shallow-water carbonate content all through the sapropel deposition are also traced by the distinct enrichment of the Sr/

Ca profile (Fig. 5i). The latter is thought to be related to enhanced fluxes of near-coastal Sr-rich aragonite or diagenetic in-situ formation of Sr-rich aragonite during sulfate reducing conditions (Thomson et al., 2004; Reitz and De Lange, 2006). A distinct increase of ascidian spicules (Fig. $6_{4–5,\ 7–8}$) during S1 deposition is however observed in the studied core (Fig. 5g) and it may have contributed in modifying the shallow water biogenic carbonate composition. The ascidian spicules are in fact composed of aragonite with high levels of Sr (i.e. up to 6.5%; Matthews, 1966) and the majority live in shallow water environment (0–50 m) (Varol and Houghton, 1996). Therefore, considering their life habitat, it is reasonable to suggest that their occurrence in our core could have resulted from a nearshore source, during the most intense flooding/run-off, mainly occurring in S1a and earlier S1b, between 8 and 7.4 ka, in agreement with the highest occurrences of *H. carteri* (Fig. 4b). The high sedimentation rates and rapid sealing of sediments soon after deposition (Houghton and Jenkins, 1988; Varol and Houghton, 1996) may have favored the preservation of ascidian spicules that in turn, although not perfectly matching the Sr/Ca profile, could have represented a further potential source for Sr-rich aragonite. Despite the low concentration of ascidian spicules (Fig. 5g), it is likely that their rather large size and high number of radial elements (Fig. $6_{4–5,\ 7–8}$) affected the Sr/Ca profile. It is noteworthy that the coccolith Sr/Ca ratio has been also suggested as a proxy for coccolithophore growth rate and productivity (e.g. Stoll and Schrag, 2000; Rickaby et al., 2007; Cavaleiro et al., 2018). However we did not detect changes in calcification in the dominant coccolith taxon *E. huxleyi* nor a relation between Sr/Ca and total coccolithophore abundance/productivity (Fig. 5b,i), suggesting that at the studied core the Sr/Ca signature was apparently no coccolith-dependent.

6. Conclusions

The high sedimentation rate and shallow depositional depth of the studied core, represented favorable conditions for the unusual preservation of calcareous and siliceous biogenic content during sapropel deposition. High resolution abundance patterns of selected calcareous nannofossil key taxa and of co-registered additional microfossil content (diatoms, siliceous sponges and ascidian spicules) allowed the reconstruction of significant changes in surface waters during the deposition of the shallow-water sapropel S1, in the Gulf of Taranto as summarized below.

- The gradual DCM development, starting from ~11 ka and lasting ~1 kyr, is coeval with the sea level rise and the gradual pre-sapropel deterioration of bottom water oxygenation in deep Adriatic records. This evidence supports the relation between sea-level rise and hydrographic changes leading towards sapropel S1 deposition.
- Enhanced surface water turbidity/run-off and nutrient availability in the subsurface waters at the core location accompany sapropel deposition between 10 and 6.5 ka, i.e. synchronous with deposition of sapropel S1 in the eastern Mediterranean. Considering that at the core location the enhanced run-off has mainly a northern source, this evidence is in favor of the relationship between the increased northern and southern borderland precipitations during sapropel S1, and strengthen the role of the mid-latitude precipitation during sapropel deposition.
- The excellent preservation of the biogenic content provides compelling evidence that diatoms, although never abundant, partially outcompete coccoliths during the highest primary productivity phase within S1a (10–8.2 ka). This feature is likely the result of high sedimentation rate at the study core.
- Short-lived reduction of river run-off/detrital input in surface water and of black organic particles into the sediment occurs at 8.2 and 7.3 ka, synchronously with brief cooling, arid spell and rapid improvement of deep-water oxygen conditions recorded in the southern Adriatic, thus revealing that these brief events are detectable at shallow water depth, both in surface and bottom environments.
- Decreased turbidity/run-off signature in surface water accompanies the final phase of S1b up to 6.5 ka, matching the decline of black particles into the sediment, which is coeval with diminished organic matter content in both eastern and central Mediterranean records.
- Multicentennial changes occur in surface-water and at the sea bottom within S1a and S1b, indicating high-frequency variability in WAC and related turbidity/low light conditions in surface waters as well as in organic carbon flux at the sea floor. This variability is thought to be associated to runoff/primary productivity which itself is thought to be related to climate, i.e. solar variability. This signal is in agreement with the supposed relation between high frequency Alpine flood variability/precipitation and solar irradiance during the Holocene.
- A distinct enrichment in ascidians during S1 implies an increase of shallow-water biogenic/detrital carbonate, whose potential source as near-coastal Sr-rich aragonite cannot be excluded, although this topic deserves further investigation.

Acknowledgments

The authors acknowledge the valuable comments and suggestions of three anonymous reviewers that resulted in an improved manuscript. This research was financially supported by Università degli Studi di Bari Aldo Moro, Fondi di Ateneo M. Marino, 2014 and benefited of instrumental upgrades from “Potenziamento Strutturale PONa3_00369 dell'Università degli Studi di Bari, Laboratorio per lo Sviluppo Integrato delle Scienze e delle TEcnologie dei Materiali Avanzati e per dispositivi innovativi (SISTEMA)”.

Appendix A. Supplementary data

Supplementary data to this article can be found online at https://doi.org/10.1016/j.palaeo.2019.109340.

References

Almogi-Labin, A., Bar-Matthews, M., Shriki, D., Kolosovsky, E., Paterne, M., Schilman, B., Ayalon, A., Aizenshtat, Z., Matthews, A., 2009. Climatic variability during the last ~90 ka of the southern and northern Levantine Basin as evident from marine records and speleothems. Quat. Sci. Rev. 28, 2882–2896.

Artegiani, A., Paschini, E., Russo, A., Bregant, D., Raicich, F., Pinardi, N., 1997. The Adriatic sea general circulation. Part I: atmospheric sea interactions and water mass structure. J. Phys. Oceanogr. 27 (8), 1492–1514.

Bar-Matthews, M., Ayalon, A., Kaufman, A., 2000. Timing and hydrological conditions of Sapropel events in the Eastern Mediterranean, as evident from speleothems, Soreq cave, Israel. Chem. Geol. 169, 145–156.

Baumann, K.-H., Bockel, B., Frenz, M., 2004. Coccolith contribution to South Atlantic carbonate sedimentation. In: Thierstein, H.R., Young, J. (Eds.), Coccolithophores From Molecular Processes to Global Impact. Springer, Berlin, pp. 367–402.

Bignami, F., Sciarra, R., Carniel, S., Santoleri, R., 2007. Variability of Adriatic Sea coastal turbid waters from SeaWiFS imagery. Journal of Geophysical Research 112, C03S10.

Boeckel, B., Baumann, K.-H., 2004. Distribution of coccoliths in surface sediments of the south-eastern South Atlantic Ocean: Ecology, preservation and carbonate contribution. Mar. Micropaleontol. 51, 3101–3320.

Boldrin, A., Langone, L., Miserocchi, S., Turchetto, M., Acri, A., 2005. Po river plume on the Adriatic continental shelf: observations on dispersion and sedimentation dynamics of dissolved and suspended matter during different river discharge rates. Mar. Geol. 222–223, 135–158.

Bond, G., Kromer, B., Beer, J., Muscheler, R., Evans, M.N., Showers, W., Hoffmann, S., Lotti-Bond, R., Hajdas, I., Bonani, G., 2001. Persistent solar influence on North Atlantic climate during the Holocene. Science 294, 2130–2136.

Bonomo, S., Cascella, A., Alberico, I., Ferraro, L., Giordano, L., Lirer, F., Vallefuoco, M., Marsella, E., 2014. Coccolithophores from near the Volturno estuary (central Tyrrhenian Sea). Mar. Micropaleontol. 111, 26–37. https://doi.org/10.1016/j.marmicro.2014.06.001.

Bukry, D., 1974. Coccoliths as paleosalinity indicators-evidence from Black Sea. AAPG Mem. 20, 353–363.

Casford, J.S.L., Rohling, E.J., Abu-Zied, R.H., Jorissen, F.J., Leng, M., Thomson, J., 2003. A dynamic concept for eastern Mediterranean circulation and oxygenation during sapropel formation. Palaeogeogr. Palaeoclimatol. Palaeoecol. 190, 103–119.

Castañeda, I.S., Schefuß, E., Pätzold, J., Sinninghe Damsté, J.S., Weldeab, S., Schouten, S., 2010. Millennial-scale sea surface temperature changes in the eastern Mediterranean

(Nile River Delta region) over the last 27,000 years. Paleoceanography 25, PA1208, doi: https://doi.org/10.1029/2009PA001740, 2010.
Castradori, D., 1993. Calcareous nannofossils and the origin of eastern Mediterranean sapropels. Paleoceanography 8 (4), 459–471.
Castradori, D., 1992. I nannofossili calcarei come strumento per lo studio biostratigrafico e paleoceanografico del Quaternario nel Mediterraneo Orientale, Ph.D. thesis, 216 pp., Univ. of Milan, Italy.
Cavaleiro, C., Voelker, A.H.L., Stoll, H., Baumann, K.H., Kulhanek, D.K., Naafs, B.D.A., Stein, R., Grützner, J., Ventura, C., Kucera, M., 2018. Insolation forcing of coccolithophore productivity in the North Atlantic during the Middle Pleistocene. Quat. Sci. Rev. 191 (2018), 318–336.
Colmenero-Hidalgo, E., Flores, J.A., Sierro, F.J., Bárcena, M.A., Löwemark, L., Schönfeld, J., Grimalt, J.O., 2004. Ocean surface water response to short-term climate changes revealed by coccolithophores from the Gulf of Cadiz (NE Atlantic) and Alboran Sea (W Mediterranean). Palaeogeogr. Palaeoclimatol. Palaeoecol. 205 (3), 317–336.
Constantin, S., Bojar, A.-V., Lauritzen, S.-E., Lundberg, J., 2007. Holocene and Late Pleistocene climate in the sub-Mediterranean continental environment: a speleothem record from Poleva cave (Southern Carpathians, Romania). Palaeogeogr. Palaeoclimatol. Palaeoecol. 243, 322–338.
Corselli, C., Principato, M.S., Maffioli, P., Crudeli, D., 2002. Changes in planktonic assemblages during sapropel S5 deposition: evidence from Urania Basin area, eastern Mediterranean. Paleoceanography 17 (3), 1029. https://doi.org/10.1029/2000PA000536.
Cramp, A., O'Sullivan, G., 1999. Neogene sapropels in the Mediterranean: a review. Mar. Geol. 153, 11–28.
Cros, L., Kleijne, A., Zelter, A., Billard, C., Young, J.R., 2000. New examples of holococcolith heterococcolith combination coccospheres and their implications for coccolithophorid Biology. Mar. Micropaleontol. 39 (1–34), 2000.
De Lange, G.J., Thomson, J., Reitz, A., Slomp, C.P., Principato, M.S., Erba, E., Corselli, C., 2008. Synchronous basin-wide formation and redox-controlled preservation of a Mediterranean sapropel. Nat. Geosci. 1, 606–610.
De Rijk, S., Rohling, E.J., Hayes, A., 1999. Onset of climatic deterioration in the eastern Mediterranean around 7 ky BP; micropalaeontological data from Mediterranean sapropel interruptions. Mar. Geol. 153, 337–343.
Desprat, S., Combourieu-Nebout, N., Essallami, L., Sicre, M.A., Dormoy, I., Peyron, O., Siani, G., Bout Roumazeilles, V., Turon, J.L., 2013. Deglacial and Holocene vegetation and climatic changes in the southern Central Mediterranean from a direct land–sea correlation. Clim. Past 9 (767–787), 2013.
Di Donato, V., Insinga, D.D., Iorio, M., Molisso, F., Rumolo, P., Cardines, C., Passaro, S., 2019. The palaeoclimatic and palaeoceanographic history of the Gulf of Taranto (Mediterranean Sea) in the last 15 ky. Glob. Planet. Chang. 172, 278–297.
Emeis, K.C., Shipboard Scientific Party of Leg 160, 1996. Paleoceanography and sapropel introduction. In: Emeis, K.C., Robertson, A.H.F., Richter, C. (Eds.), Proc. ODP Init. Repts. 160. College Station, TX, pp. 21–27.
Emeis, K.-C., Schulz, H.-M., Struck, U., Sakamoto, T., Doose, H., Erlenkeuser, H., Howell, M., Kroon, D., Paterne, M., 1998. Stable isotope and temperature records of sapropels from ODP Sites 964 and 967: constraining the physical environment of sapropel formation in the Eastern Mediterranean Sea. In: Robertson, A.H.F. (Ed.), Proc. ODP, Sci. Res., vol. 160. Ocean Drilling Program, College Station, TX, pp. 309–331.
Ferreira, J., Cachão, M., González, R., 2008. Reworked calcareous nannofossils as ocean dynamic tracers: the Guadiana shelf case study (SW Iberia). Estuar. Coast. Shelf Sci. 79 (1), 59–70.
Filippidi, A., De Lange, G.J., 2019. Eastern Mediterranean deep water formation during Sapropel S1: a reconstruction using geochemical records along a bathymetric transect in the adriatic outflow region. Paleoceanography and Paleoclimatology 34, 409–429. https://doi.org/10.1029/2018PA003459.
Filippidi, A., Triantaphyllou, M.V., De Lange, G.J., 2016. Eastern-Mediterranean ventilation variability during sapropel S1 formation, evaluated at two sites influenced by deep-water formation from Adriatic and Aegean Seas. Quat. Sci. Rev. 144, 95–106.
Flores, J.-A., Sierro, F.J., 1997. Revised technique for calculation of calcareous nannofossil accumulation rates. Micropaleontology 43 (3), 321–324.
Flores, J.A., Sierro, F.J., Francés, G., Vàzquez, A., Zamarrefio, I., 1997. The last 100,000 years in the western Mediterranean: sea surface water and frontal dynamics as revealed by Coccolithophores. Mar. Micropaleontol. 29, 351–366.
Frisia, S., Borsato, A., Mangini, A., Spoetl, C., Madonia, G., Sauro, U., 2006. Holocene climate variability in Sicily froma discontinuous stalagmite record and the Mesolithic to Neolithic transition. Quat. Res. 66, 388–400.
Gasse, F., 2000. Hydrological changes in the African tropics since the last glacial maximum. Quat. Sci. Rev. 19, 189–211.
Gasse, F., 2002. Diatom-inferred salinity and carbonate oxygen isotopes in Holocene water bodies of the western Sahara and Sahel (Africa). Quat. Sci. Rev. 21, 737–767.
Giunta, S., Negri, A., Morigi, C., Capotondi, L., Combourieu-Nebout, N., Emeis, K., Sangiorgi, F., Vigliotti, L., 2003. Coccolithophorid ecostratigraphy and multiproxy paleoceanographic reconstruction in the Southern Adriatic Sea during the last deglacial time (Core AD91-17). Palaeogeogr. Palaeoclimatol. Palaeoecol. 190, 39–59.
Giunta, S., Negri, A., Maffioli, P., Sangiorgi, F., Capotondi, L., Morigi, C., Principato, M.S., Corselli, C., 2006. Phytoplankton dynamics in the eastern Mediterranean Sea during Marine Isotopic Stage 5e. Palaeogeogr. Palaeoclimatol. Palaeoecol. 235, 28–47.
Giunta, S., Morigi, C., Negri, A., Guichard, F., Lericolais, G., 2007. Holocene biostratigraphy and paleoenvironmental changes in the Black Sea based on calcareous nannoplankton. Mar. Micropaleontol. 63 (1–2), 91–110.
Goudeau, M.-L.S., Reichart, G.-J., Wit, J.C., de Nooijer, L.J., Grauel, A.-L., Bernasconi, S.M., de Lange, G.J., 2015. Seasonality variations in the Central Mediterranean during climate change events in the Late Holocene. Palaeogeogr. Palaeoclimatol. Palaeoecol. 418, 304–318.
Goudeau, M.-L.S., Grauel, A.-L., Bernasconi, S., De Lange, G.J., 2013. Provenance of surface sediments along the southeastern Adriatic coast off Italy: an overview. Estuarine Coastal and Shelf Science 134, 45–56. https://doi.org/10.1016/j.ecss.2013.09.009.
Goudeau, M.-L.S., Grauel, A.-L., Tessarolo, C., Leider, A., Chen, L., Bernasconi, S.M., Versteegh, G.J.M., Zonneveld, K.A.F., Boer, W., Alonso-Hernandez, C.M., De Lange, G.J., 2014. The Glacial-interglacial transition and Holocene environmental changes in sediments from the Gulf of Taranto, central Mediterranean. Mar. Geol. 348, 88–102.
Gran, H.H., Braarud, T., 1935. A quantitative study of the phytoplankton in the Bay of Fundy and the Gulf of Maine (including observations on hydrography, chemistry and turbidity). Journal of Biology Board of Canada 1, 279–467.
Grant, K.M., Rohling, E.J., Bar-Matthews, M., Ayalon, A., Medina-Elizalde, M., Bronk Ramsey, C., Satow, C., Roberts, A.P., 2012. Rapid coupling between ice volume and polar temperature over the past 150 kyr. Nature 491, 744–747.
Grant, K.M., Grimm, R., Mikolajewicz, U., Marino, G., Ziegler, M., Rohling, E.J., 2016. The timing of Mediterranean sapropel deposition relative to insolation, sea-level and African monsoon changes. Quat. Sci. Rev. 140, 125–141. https://doi.org/10.1016/j.quascirev.2016.03.026.
Grauel, A.-L., Leider, A., Goudeau, M.-L.S., Müller, I.A., Bernasconi, S.M., Hinrichs, K.-U., De Lange, G.J., Zonneveld, K.A.F., Versteegh, G.J.M., 2013a. What do SST really tell us? A high-resolution multiproxy (UK'37, TEXH86 and foraminifera δ18O) study in the Gulf of Taranto, central Mediterranean Sea. Quat. Sci. Rev. 73, 115–131.
Grauel, A.-L., Goudeau, M.-L., de Lange, G.J., Bernasconi, S.M., 2013b. Climate of the past 2500 years in the Gulf of Taranto, central Mediterranean Sea: a high-resolution climate reconstruction based on δ18O and δ13C of Globigerinoides ruber (white). The Holocene 23 (10), 1440–1446. https://doi.org/10.1177/0959683613493937.
Grbec, B., Vilibić, I., Bajić, A., Morović, M., Bec Paklar, G., Matić, F., Dadić, V., 2007. Response of the Adriatic Sea to the atmospheric anomaly in 2003. Ann. Geophys. 25, 835–846.
Grelaud, M., Marino, G., Ziveri, P., Rohling, E.J., 2012. Abrupt shoaling of the nutricline in response to massive freshwater flooding at the onset of the last interglacial sapropel event. Paleoceanography 27.
Grimm, R., Maier-Reimer, E., Mikolajewicz, U., Schmiedl, G., Müller-Navarra, K., Adloff, F., Grant, K.M., Ziegler, M., Lourens, L.J., Emeis, K.-C., 2015. Late glacial initiation of Holocene eastern Mediterranean sapropel formation. Nat. Commun. 6.
Hagino, K., Okada, H., Matsuoka, H., 2005. Coccolithophore assemblages and morphotypes of Emiliania huxleyi in the boundary zone between the cold Oyashio and warm Kuroshio currents off the coast of Japan. Mar. Micropaleontol. 55, 19–47.
Hennekam, R., Jilbert, T., Schnetger, B., de Lange, G.J., 2014. Solar forcing of Nile discharge and sapropel S1 formation in the early to middle Holocene eastern Mediterranean. Paleoceanography 29, 343–356.
Houghton, S.D., Jenkins, D.G., 1988. Subtropical microfossil indicators from the Pliocene Celtic Sea. Mar. Geol. 7 (9), 119–126.
Howell, M.W., Thunell, R.C., 1992. Organic carbon accumulation in Bannock Basin: evaluating the role of productivity in the formation of eastern Mediterranean sapropels. Mar. Geol. 103, 461–471.
Incarbona, A., Di Stefano, E., 2019. Calcareous nannofossil palaeoenvironmental reconstruction and preservation in sapropel S1 at the Eratosthenes Seamount (Eastern Mediterranean). Deep-Sea Research Part II 164, 206–215. https://doi.org/10.1016/j.dsr2.2018.10.004.
Incarbona, A., Ziveri, P., Sabatino, N., Manta, D.S., Sprovieri, M., 2011. Conflicting coccolithophore and geochemical evidence for productivity levels in the Eastern Mediterranean sapropel S1. Mar. Micropaleontol. 81 (3–4), 131–143.
Jilbert, T., Reichart, G.J., Mason, P., de Lange, G.J., 2010. Short-time-scale variability in ventilation and export productivity during the formation of Mediterranean sapropel S1. Paleoceanography 25, PA4232. https://doi.org/10.1029/2010PA001955.
Jordan, R.W., Cros, L., Young, J.R., 2004. A revised classification scheme for living haptophytes. Micropaleontology 50, 55–79. https://doi.org/10.2113/50.Suppl_1.55.
Kemp, A.E.S., Pearce, R.B., Koizumi, I., Pike, J., Rance, S.J., 1999. The role of mat-forming diatoms in the formation of Mediterranean sapropels. Nature 398, 57–61.
Kidd, R.B., Cita, M.B., Ryan, W.B.F., 1978. Stratigraphy of Eastern Mediterranean sapropel sequences recovered during DSDP Leg 42A and their paleoenvironmental significance. Init. Rep. DSDP Leg 42, 421–443.
Kotthoff, U., Pross, J., Müller, U.C., Peyron, O., Schmiedl, G., Schulz, H., Bordon, A., 2008. Climate dynamics in the borderlands of the Aegean Sea during formation of sapropel S1 deduced from a marine pollen record. Quat. Sci. Rev. 27, 832–845.
Krom, M.D., Kress, N., Brenner, S., Gordon, L.I., 1991. Phosphorus limitation of primary productivity in the eastern Mediterranean sea. Limnol. Oceanogr. 36, 424–432.
Kuhnt, T., Schmiedl, G., Ehrmann, W., Hamann, Y., Hemleben, C., 2007. Deep-sea ecosystem variability of the Aegean Sea during the past 22 kyr as revealed by Benthic Foraminifera. Mar. Micropaleontol. 64, 141–162.
Ludwig, J. R., Volcani, B. E., 1986. A molecular biology approach to understanding silicon metabolism in diatoms, in Biomineralization, in Leadbeater, B. S. C., Riding, R., (Eds.), Lower Plants and Animals, Syst. Assoc. Spec. vol. 30, Clarendon, Oxford, UK, pp. 315–326.
Magny, M., Vannière, B., Calo, C., Millet, L., Leroux, A., Peyron, O., Zanchetta, G., La Mantia, T., Tinner, W., 2011. Holocene hydrological changes in south-western Mediterranean as recorded by lake-level fluctuations at Lago Preola, a coastal lake in southern Sicily. Italy. Quat. Sci. Rev. 30, 2459–2475.
Malanotte-Rizzoli, P., Manca, B., Ribera, D'Alcalà M., Theocharis, A., Bergamasco, A., Bregant, D., Budillon, G., Civitarese, G., Georgopoulos, D., Michelato, A., Sansone, E., Scarazzato, P., Souvermezoglou, E., 1997. A synthesis of the Ionian Sea hydrography, circulation and water mass pathway during POEM-Phase I. Prog. Oceanography 39, 153–204.
Malinverno, E., Maffioli, P., Corselli, C., De Lange, G.J., 2014. Present-day fluxes of Coccolithophores and diatoms in the pelagic Ionian Sea. J. Mar. Syst. 132, 13–27.

Marino, G., Rohling, E.J., Sangiorgi, F., Hayes, A., Casford, J.L., Lotter, A.F., Kucera, M., Brinkhuis, H., 2009. Early and middle Holocene in the Aegean Sea: interplay between high and low latitude climate variability. Quat. Sci. Rev. 28 (27–28), 3246–3262.
Martrat, B., Jimenez-Amat, P., Zahn, R., Grimalt, J.O., 2014. Similarities and dissimilarities between the last two deglaciations and interglaciations in the North Atlantic region. Quat. Sci. Rev. 99, 122–134.
Matthews, R.K., 1966. Genesis of recent lime mud in southern British Honduras. J. Sediment. Petrol. 36 (2), 428–454.
Mercone, D., Thomson, J., Croudace, I.W., Siani, G., Paterne, M., Troelstra, S., 2000. Duration of S1, the most recent sapropel in the eastern Mediterranean Sea, as indicated by accelerator mass spectrometry radiocarbon and geochemical evidence. Paleoceanography 15, 336–347.
Mercone, D., Thomson, J., Abu-Zied, R.H., Croudace, I.W., Rohling, E.J., 2001. Highresolution geochemical and micropalaeontological profiling of the most recent eastern Mediterranean sapropel. Mar. Geol. 177, 25–44. https://doi.org/10.1016/S0025-3227(01)00122-0.
Milligan, T.G., Cattaneo, A., 2007. Sediment dynamics in the western Adriatic Sea: from transport to stratigraphy. Cont. Shelf Res. 27, 287–295.
Myers, P.G., Haines, K., Rohling, E.J., 1998. Modelling the paleocirculation of the Mediterranean: the Last Glacial Maximum and the Holocene with emphasis on the formation of sapropel S1. Paleoceanography 13 (6), 586–606.
Narciso, À., Flores, J.-A., Cachão, M., Sierro, F.J., Colmenero-Hidalgo, E., Piva, A., Asioli, A., 2010. Sea surface dynamics and coccolithophore behaviour during sapropel deposition of Marine Isotope Stage 7, 6 and 5 in the Western Adriatic Sea. Rev. Esp. Micropaleontol. 42 (3), 345–358.
Narciso, A., Flores, J.A., Cachão, M., Piva, A., Asioli, A., Andersen, N., Schneider, R., 2013. Late Glacial–Holocene transition in the southern Adriatic Sea: Coccolithophore and Foraminiferal evidence. Micropaleontology 58 (6), 523–538.
Negri, A., Giunta, S., 2001. Calcareous nannofossil paleoecology in the sapropel S1 of the eastern Ionian sea: paleoceanography implications. Palaeogeogr. Palaeoclimatol. Palaeoecol. 169, 101–112.
Negri, A., Capotondi, L., Keller, J., 1999. Calcareous nannofossils, planktic foraminifers and oxygen isotope in the late Quaternary sapropels of the Ionian Sea. Mar. Geol. 157, 84–99.
Nijenhuis, I.A., Schenau, S.J., Van der Weijden, C.H., Hilgen, F.J., Lourens, L.J., Zachariasse, W.J., 1996. On the origin of upper Miocene sapropelites: a case study from the Faneromeni section, Crete (Greece). Paleoceanography 11 (5), 633–645.
Olausson, E., 1961. Studies of deep-sea cores. Rep. Swed. Deep-Sea Exped. 1947–1948 (8), 335–391.
van Os, B.J.H., Lourens, L.J., Hilgen, F.J., de Lange, G.J., Beaufort, L., 1994. The formation of Pliocene sapropels and carbonate cycles in the Mediterranean: diagenesis, dilution and productivity. Paleoceanography 9, 601–617.
Pierre, C., 1999. The oxygen and carbon isotope distribution in the Mediterranean water masses. Mar. Geol. 153, 41–55.
Poulain, P.-M., 2001. Adriatic Sea surface circulation as derived from drifter data between1990 and 1999. J. Mar. Syst. 29, 3–32.
Poulton, A.J., Holligan, P.M., Charalampopoulou, A., Adey, T.R., 2017. Coccolithophore ecology in the tropical and subtropical Atlantic Ocean: new perspectives from the Atlantic meridional transect (AMT) programme. Prog. Oceanogr. 158, 150–170.
Principato, M.S., Giunta, S., Corselli, C., Negri, A., 2003. Late Pleistocene/Holocene planktonic assemblages in three box-cores from the Mediterranean Ridge are (W–SW of Crete): paleoecological and paleoceanographic reconstruction of sapropel S1 interval. Palaeogeogr. Palaeoclim. Palaeoecol. 190, 61–77.
Principato, M., Crudeli, D., Ziveri, P., Slomp, C., Corselli, C., Erba, E., De Lange, G.J., 2006. Phyto- and zooplankton paleofluxes during the deposition of sapropel S1 (eastern Mediterranean): Biogenic carbonate preservation and paleoecological implications. Palaeogeogr. Palaeoclimatol. Palaeoecol. 235, 8–27.
Reitz, A., De Lange, G.J., 2006. Abundant Sr-rich aragonite in eastern Mediterranean sapropel S1: Diagenetic versus detrital/biogenic origin. Palaeogeogr. Palaeoclimatol. Palaeoecol. 235, 135–148.
Rickaby, R.E.M., Bard, E., Sonzogni, C., Rostek, F., Beaufort, L., Barker, S., Rees, G., Schrag, D.P., 2007. Coccolith chemistry reveals secular variations in the global ocean carbon cycle? Earth Planet Sci. Lett. 253, 83–95. https://doi.org/10.1016/j.epsl.2006.10.016.
Rohling, E.J., 1994. Review and new aspects concerning the formation of Eastern Mediterranean sapropels. Mar. Geol. 122, 1–28.
Rohling, E.J., Gieskes, W.W.C., 1989. Late Quaternary changes in Mediterranean Intermediate Water density and formation rate. Paleoceanography 4, 531–545.
Rohling, E.J., Hilgen, F.J., 1991. The eastern Mediterranean climate at times of sapropel formation: a review. Geol. En. Mijnb. 70, 253–264.
Rohling, E.J., Pälike, H., 2005. Centennial-scale climate cooling with a sudden cold event around 8,200 years ago. Nature 434, 975–979.
Rohling, E., Jorissen, F., De Stigter, H., 1997. 200 year interruption of Holocene sapropel formation in the Adriatic Sea. J. Micropalaeontol. 16, 97–108.
Rohling, E.J., Cane, T.R., Cooke, S., Sprovieri, M., Bouloubassi, I., Emeis, K.C., Schiebel, R., Kroon, D., Jorissen, F.J., Lorre, A., Kemp, A.E.S., 2002. African monsoon variability during the previous interglacial maximum. Earth Planet. Sci. Lett. 202, 61–75.
Rohling, E.J., Sprovieri, M., Cane, T., Casford, J.S.L., Cooke, S., Bouloubassi, I., Emeis, K.C., Schiebel, R., Rogerson, M., Hayes, A., Jorissen, F.J., Kroon, D., 2004. Reconstructing past planktic foraminiferal habitats using stable isotope data: a case history for Mediterranean sapropel S5. Mar. Micropaleontol. 50, 89–123.
Rohling, E., Marino, G., Grant, K., 2015. Mediterranean climate and oceanography, and the periodic development of anoxic events (sapropels). Earth Sci. Rev. 143, 62–97.
Rossi, S., Auroux, C., Mascle, J., 1983. The Gulf of Taranto (Southern Italy): Seismic stratigraphy and shallow structure. Mar. Geol. 51, 327–346.
Rossignol-Strick, M., 1985. Mediterranean Quaternary sapropels, an immediate response of the African monsoon to variation of insolation. Palaeogeogr. Palaeoclimatol. Palaeoecol. 49, 237–263.
Rossignol-Strick, M., 1987. Rainy periods and bottom water stagnation initiating brine accumulation and metal concentrations: 1. the Late Quaternary. Paleoceanography 2, 333–360.
Rossignol-Strick, M., 1999. The Holocene climatic optimum and pollen records of sapropel 1 in the eastern Mediterranean, 9000–6000 BP. Quat. Sci. Rev. 18, 515–530.
Rossignol-Strick, M., Nesteroff, W., Olive, P., Vergnaud-Grazzini, C., 1982. After the deluge: Mediterranean stagnation and sapropel formation. Nature 295, 105–110.
Sancetta, C., 1994. Mediterranean sapropels: seasonal stratification yields high production and carbon flux. Paleoceanography 9, 195–196.
Sellschopp, J., Álvarez, A., 2003. Dense low-salinity outflow from the Adriatic Sea under mild (2001) and strong (1999) winter conditions. J. Geophys. Res. 108 (C9), 8104.
Siani, G., Magny, M., Paterne, M., Debret, M., Fontugne, M., 2013. Paleohydrology reconstruction and Holocene climate variability in the south Adriatic sea. Clim. Past 9, 499–515.
Spötl, C., Nicolussi, K., Patzelt, G., Boch, R., 2010. Humid climate during deposition of sapropel 1 in the Mediterranean sea: assessing the influence on the Alps. Glob. Planet. Change 71, 242–248.
Stoll, H.M., Schrag, D.P., 2000. Coccolith Sr/Ca as a new indicator of coccolithophorid calcification and growth rate. Geochem. Geophys. Geosyst. 1 (5). https://doi.org/10.1029/1999GC000015.
Tesi, T., Asioli, A., Minisini, D., Maselli, V., Dalla Valle, G., Gamberi, F., Langone, L., Cattaneo, A., Montagna, P., Trincardi, F., 2017. Large-scale response of the Eastern Mediterranean thermohaline circulation to African monsoon intensification during sapropel S1 formation. Quat. Sci. Rev. 159, 139–154.
Thomson, J., Crudeli, D., De Lange, G.J., Slomp, C., Erba, E., Corselli, C., 2004. Florisphaera profunda and the origin and diagenesis of carbonate phases in eastern Mediterranean sapropel units. Paleoceanography 19, PA3003.
Toucanne, S., Minto'o, C.M.A., Fontanier, C., Bassetti, M.-A., Jorry, S.J., Jouet, G., 2015. Tracking rainfall in the northern Mediterranean borderlands during sapropel deposition. Quat. Sci. Rev. 129, 178–195.
Triantaphyllou, M.V., 2014. Coccolithophore assemblages during the Holocene climatic optimum in the NE Mediterranean (Aegean and northern Levantine Seas, Greece): paleoceanographic and paleoclimatic implications. Quat. Int. 345, 56–67.
Triantaphyllou, M.V., Antonarakou, A., Kouli, K., Dimiza, M.D., Kontakiotis, G., Papanikolaou, M.D., Ziveri, P., Mortyn, P.G., Lianou, V., Lykousis, V., Dermitzakis, M.D., 2009. Late Glacial-Holocene ecostratigraphy of the south-eastern Aegean Sea, based on plankton and pollen assemblages. Geo-Mar. Lett. 29, 249–267.
Triantaphyllou, M.V., Antonarakou, A., Dimiza, M.D., Anagnostou, C., 2010. Calcareous nannofossil and planktonic foraminiferal distributional patterns during deposition of sapropels S6, S5 and S1 in the Libyan Sea (Eastern Mediterranean). Geo-Mar. Lett. 30, 1–13.
Triantaphyllou, M.V., Gogou, A., Dimiza, M.D., Kostopoulou, S., Parinos, C., Roussakis, G., Geraga, M., Bouloubassi, I., Fleitmann, D., Zervakis, V., Velaoras, D., Diamantopoulou, A., Sampatakaki, A., Lykousis, V., 2016. Holocene climatic optimum centennial-scale paleoceanography in the NE Aegean (Mediterranean Sea). Geo-Mar. Lett. 36, 51–66.
Turchetto, M., Boldrin, A., Langone, L., Miserocchi, S., Tesi, T., Foglini, F., 2007. Particle transport in the Bari Canyon (southern Adriatic Sea). Mar. Geol. 246, 231–247.
Varol, O., Houghton, S.D., 1996. A review and classification of fossil didemnid ascidian spicules. J. Micropaleontol. 15, 135–149.
Vilibić, I., Orlić, M., 2002. Adriatic water masses, their rates of formation and transport through the Otranto Strait. Deep-Sea Research I 49, 1321–1340.
Weldeab, S., Menke, V., Schmiedl, G., 2014. The pace of East African monsoon evolution during the Holocene. Geophys. Res. Lett. 41, 1724–1732.
Winter, A., Jordan, R.W., Roth, P.H., 1994. Biogeography of living Coccolithophores in ocean waters. In: Winter, A., Siesser, W.G. (Eds.), Coccolithophores. Cambridge University Press, London, pp. 161–178.
Wirth, S.B., Glur, L., Gilli, A., Anselmetti, F.S., 2013. Holocene flood frequency across the Central Alps – solar forcing and evidence for variations in North Atlantic atmospheric circulation. Quat. Sci. Rev. 80, 112–128. https://doi.org/10.1016/j.quascirev.2013.09.002.
Wu, J., Boning, P., Pahnke, K., Tachikawa, K., de Lange, G.J., 2016. Unraveling North-African riverine and eolian contributions to central Mediterranean sediments during Holocene sapropel S1 formation. Quat. Sci. Rev. 152, 31–48.
Wu, J., Filippidi, A., Davies, G.R., de Lange, G.J., 2018. Riverine supply to the eastern Mediterranean during last interglacial sapropel S5 formation: a basin-wide perspective. Chem. Geol. 485, 74–89.
Young, J.R., Geisen, M., Cros, L., Kleijne, A., Sprengel, C., Probert, I., Østergaard, J., 2003. A guide to extant coccolithophore taxonomy. J. Nannoplankt Res. 1 (Spec. Iss.), 1–125.
Zanchetta, G., Drysdale, R.N., Hellstrom, J.C., Fallick, A.E., Isola, I., Gagan, M.K., Pareschi, M.T., 2007. Enhanced rainfall in the Western Mediterranean during deposition of sapropel S1: stalagmite evidence from Corchia cave (Central Italy). Quat. Sci. Rev. 26, 279–286.
Ziegler, M., Jilbert, T., de Lange, G.J., Lourens, L.J., Reichart, G.J., 2008. Bromine counts from XRF scanning as an estimate of the marine organic carbon content of sediment cores. Geochem. Geophys. Geosyst. 9, Q05009. https://doi.org/10.1029/2007GC001932.